

Diruthenium(I,I) saccharinate complexes: Synthesis, molecular structure, and evaluation as catalysts for carbenoid reactions of diazoacetates

Stefan Buck, Gerhard Maas *

Abteilung Organische Chemie I, Universität Ulm, Albert-Einstein-Allee 11, D-89081 Ulm, Germany

Received 31 January 2006; accepted 10 February 2006

Available online 6 March 2006

Abstract

The dinuclear ruthenium complexes $[\text{Ru}_2(\mu\text{-sac})_2(\text{CO})_6]$ (**1**), $[\text{Ru}_2(\mu\text{-sac})_2(\text{CH}_3\text{CN})_2(\text{CO})_4]$ (**3**), $[\text{Ru}_2(\mu\text{-sac})_2(\text{CO})_5(\text{PPh}_3)]$ (**4**) and $[\text{Ru}_2(\mu\text{-sac})_2(\text{CO})_4(\text{PPh}_3)_2]$ (**5**) as well as the tetranuclear ruthenium complex $[\text{Ru}_2(\mu\text{-sac})_2(\text{CO})_5]_2$ (**2**) (sac = saccharinate, $\text{C}_7\text{H}_4\text{NO}_3\text{S}^-$) were synthesized starting from $\text{Ru}_3(\text{CO})_{12}$ and saccharin. X-ray crystal structure analysis of **1**, **3A** \times *p*-xylene, **4** \times CH_2Cl_2 and **5** \times $3\text{CH}_2\text{Cl}_2$ showed that the Ru_2^{2+} core is bridged through the amidate moieties of the two saccharinate ligands, with a head–tail arrangement in complexes **1**, **3A** and **5**, and a head–head arrangement in **4**. For complex **3**, an equilibrium mixture of the head–head regioisomer **3A** and a second species **3b** exists in solution. Complexes **1** and **2** are suitable catalysts for the cyclopropanation of nucleophilic alkenes (styrene, cyclohexene and 2-methyl-2-butene) with methyl diazoacetate.

© 2006 Elsevier B.V. All rights reserved.

Keywords: Ruthenium(I) complexes; Saccharin; Catalysts; Cyclopropanation; Diazo compounds

1. Introduction

Carbenoid reactions of aliphatic diazo compounds represent valuable tools in synthetic organic chemistry [1,2]. These transformations are catalyzed effectively and efficiently by a variety of catalysts based in particular on copper and rhodium. Recently, ruthenium complexes, with different oxidation states of the metal and a variety of ligand systems, have emerged as novel catalysts for diazo decomposition and carbene transfer reactions. While the majority of studies so far have focused on alkene cyclopropanation reactions [3], increasing attention is now given to other carbenoid reactions, e.g., insertion into C–H [4] and X–H [5] bonds, formation of ylides (carbonyl ylides [6], P-ylides with subsequent aldehyde olefination [7], and N-ylides [8]), and formation of carbene dimers [9].

Almost all of the rhodium catalysts which have been successfully applied to carbenoid transformations of diazo

compounds constitute dinuclear rhodium(II) catalysts of the type Rh_2L_4 , where L represents a bridging anionic ligand such as carboxylate, amidate, phosphate, or $\text{C}_6\text{H}_4\text{-PPh}_2$ [1]. Inspired by the success and versatility of these rhodium complexes, we have investigated structurally related dinuclear ruthenium complexes with the Ru_2^{2+} core and the general composition $[\text{Ru}_2(\mu\text{-L}^1)(\text{CO})_4\text{L}^2\text{L}^3]$, where L^1 is a bidentate bridging ligand such as carboxylate [10,11], triazenide [12] and pyridin-2-olate [11] while L^2 and L^3 represent axial ligands at one or both ruthenium atoms. Up to present, the anion of saccharin (*o*-sulfobenzamide, 1,2-benzisothiazol-3(2*H*)-one) has not been considered as a bidentate ligand in catalytically active dinuclear Rh or Ru complexes, although saccharin features an amidate-like moiety that is reminiscent of several excellent tetrakis(amidato)-dirhodium catalysts. In fact, the multifunctional saccharinate anion (sac) can engage in several different coordination modes [13], of which the simple N-coordination is the most common one [14]. Notably, complexes in which saccharinate acts as a bidentate ligand via the amidate (N–C=O) fragment have been reported only

* Corresponding author.

E-mail address: gerhard.maas@uni-ulm.de (G. Maas).

occasionally. This coordination motif has been found in mononuclear lead(II) complexes [15] and dinuclear copper complexes [13a,16]. Dinuclear chromium complexes of the type $[\text{Cr}_2(\text{sac})_4]$ or $[\text{Cr}_2(\text{sac})_4\text{L}_2]$ [17], where four saccharinate ligands bridge a Cr(II)–Cr(II) core, represent the closest structural analogy to the ruthenium complexes which are described in this communication.

2. Results and discussion

2.1. Preparation of ruthenium complexes 1–5

Following the established method for the preparation of other dinuclear ruthenium(I,I) complexes, the ruthenium saccharinate complexes were prepared from $\text{Ru}_3(\text{CO})_{12}$ and the protonated form of the bridging ligand (Hsac). When $\text{Ru}_3(\text{CO})_{12}$ and saccharin (1:3 stoichiometry) were heated in toluene at 90 °C for 36 h, the complex $[\text{Ru}_2(\mu\text{-sac})_2(\text{CO})_6]$ (**1**) was obtained as an air- and moisture-stable pale yellow solid in 80% yield (Scheme 1). The compound is fairly soluble in noncoordinating organic solvents such as dichloromethane. The composition of **1** is in agreement with the elemental analysis, and the head–tail arrangement of the two sac ligands (1,1 regioisomer) as well as the presence of an axial CO ligand at each ruthenium atom is uncovered by the results of an XRD structure determination (see Section 2.2).

It should be noted that the thermal stability of complexes of the type $[\text{Ru}_2(\mu\text{-L})_2(\text{CO})_6]$ varies considerably: While **1** as well as related triazenide [12] and pyrazolate [18] complexes can be isolated as stable complexes, the pyridonate ($[\text{Ru}_2(\mu\text{-Opy})_2(\text{CO})_6]$ [19]) and carboxylate complexes ($[\text{Ru}_2(\mu\text{-OOCR})_2(\text{CO})_6]$ [20]) readily lose their axial CO ligands in the absence of a CO atmosphere. On the other hand, complex **1** splits off carbon monoxide when kept in boiling toluene (110 °C) and is transformed into an air- and moisture-stable yellow powder. The same compound was obtained in 89% yield when $\text{Ru}_3(\text{CO})_{12}$ and saccharin were heated in boiling toluene for 5 h. The product was completely insoluble in pentane or cyclohexane and only barely soluble in chloroalkanes. Although no final structural proof could be obtained so far, we assume that the product represents the tetranuclear ruthenium complex $[\text{Ru}_2(\mu\text{-sac})_2(\text{CO})_5]_2$ (**2**), a coordination dimer of a dinuclear ruthenium complex. Recently, we have established the structure of an analogous complex with fluoropyridonate rather than saccharinate ligands [21]. Obviously, the thermal conversion of **1** into **2** proceeded by expulsion of one axial CO ligand, rearrangement from the head–tail (0,2) to the head–head (1,1) regioisomer and dimerization across a Ru–O bond. Steric interactions with the SO_2 group of the second sac ligand are likely to prevent the analogous dimerization of the head–tail regioisomer.

As expected, suitable Lewis bases were able to cleave the coordination dimer **2** (Scheme 1). Thus, exposure of **2** to acetonitrile furnished the yellow complex $[\text{Ru}_2(\mu\text{-sac})_2(\text{CH}_3\text{CN})_2(\text{CO})_4]$ (**3**) which in solution existed as an

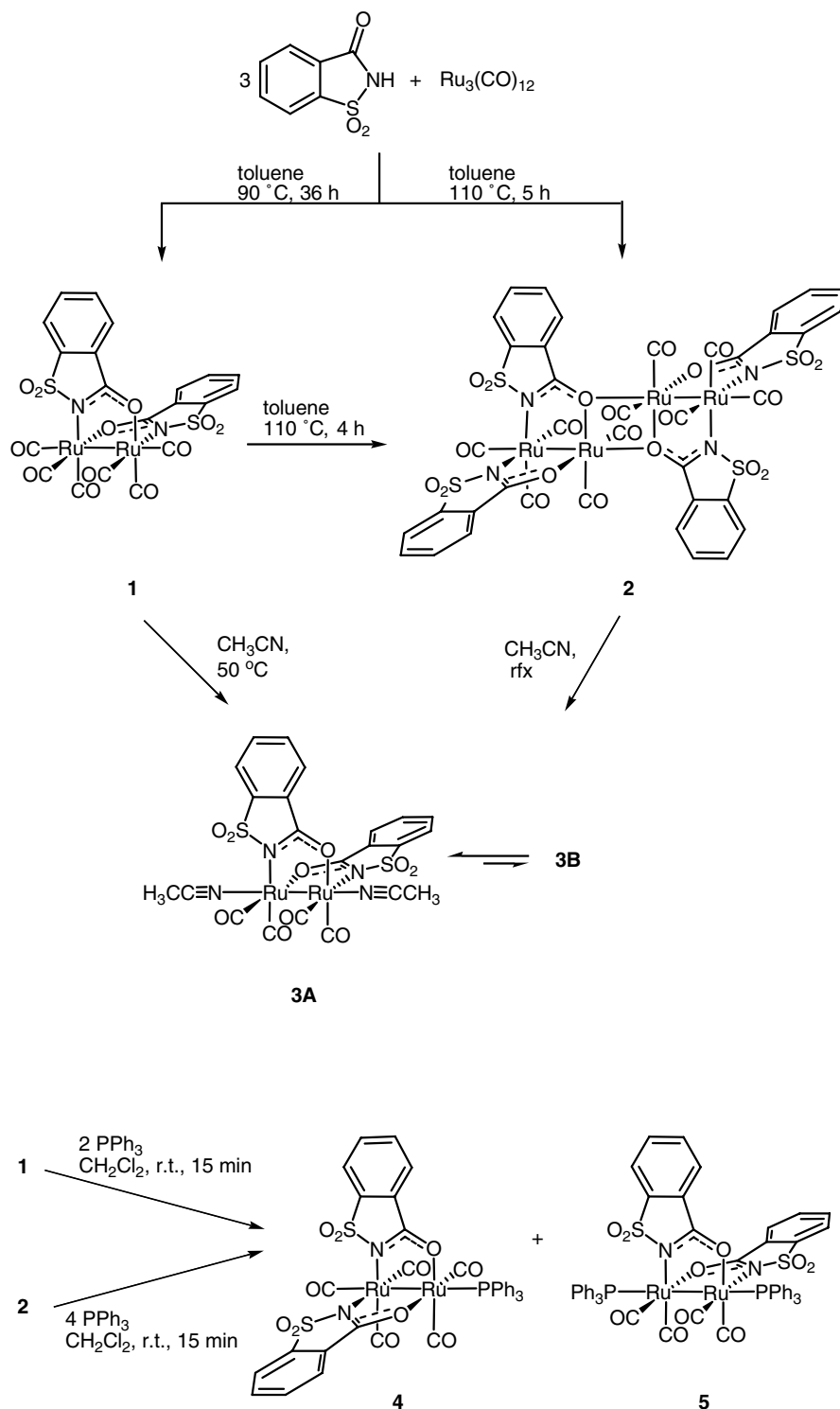
equilibrium mixture of two species as indicated by the NMR spectra. Due to incomplete signal separation of the ^1H signals, the ratio could be determined only approximately as **A**:**B** \approx 2.9:1 at 295 K, and it appeared that this ratio changed only slightly between 243 and 328 K. Crystallization of **3** from $\text{CH}_3\text{CN}/p$ -xylene for an XRD analysis furnished the head–tail regioisomer **3A**. It could not be clarified so far whether the minor species **3B**, which was detected in solution and which has ^{13}C and ^1H NMR chemical shifts quite similar to those of **3A** ($\Delta\delta$ less than 0.8 ppm), is the head–head isomer or a different species. Compound **3** was also obtained by heating of hexacarbonyl complex **1** in acetonitrile solution. Efforts to separate **3A** and **3B** by chromatography on silica gel were fruitless: Although two fractions with different R_f values could be isolated, their NMR spectra were identical with those before chromatography.

Short treatment of **2** with triphenylphosphane led to a mixture of the yellow complex $[\text{Ru}_2(\mu\text{-sac})_2(\text{CO})_5(\text{PPh}_3)]$ (**4**) and the orange complex $[\text{Ru}_2(\mu\text{-sac})_2(\text{CO})_4(\text{PPh}_3)_2]$ (**5**). Crystallization from dichloromethane/pentane yielded a mixture of yellow and orange crystals which could be separated manually. XRD analysis established the different constitution of both compounds and showed that the head–head arrangement of the two sac ligands is present in **4**, while **5** constitutes the head–tail regioisomer. A ^{31}P NMR control experiment showed that **4** ($\delta_{\text{P}} = 22.0$ ppm) was slowly converted into **5** ($\delta_{\text{P}} = 14.1$ ppm) in the presence of PPh_3 : starting from equimolar amounts of **4** and PPh_3 in CDCl_3 , the **4**:**5** ratio was 5:1 after 1 h and 4:1 after 18 h; combination of **4** with two equivalents of PPh_3 furnished a 0.4:1 mixture of **4** and **5** after 1 h. A mixture of **4** and **5** was also obtained when hexacarbonyl complex **1** was treated with PPh_3 (Scheme 1).

For related 6-halogenopyridonate complexes, we have recently observed that the interconversion of head–head and head–tail regioisomers occurs quite easily and that the result depends on the axial ligands at the two ruthenium centers [22]. The isolation of **4**, with one axial CO ligand, indirectly confirms the proposed structure of the dimeric complex **2** and excludes a polymeric *catena* structure of the type $[\text{Ru}_2(\mu\text{-L})_2(\text{CO})_4]_n$ (i.e., Ru–O coordination at both ruthenium centers) which has been found with bridging carboxylate as well as pyridonate ligands [23].

Complexes **1**–**5** were also characterized spectroscopically (Table 1). In the IR spectra, the carbonyl absorptions of **3** and **5** show the typical pattern of a sawhorse-shaped $\text{M}_2(\text{CO})_4$ unit (see, e.g., literature [19,20,24,25a]), while the hexacarbonyl and pentacarbonyl complexes (**1**, **2**, **4**) show a more complex absorption pattern. Absorptions at high wavenumbers ($2083\text{--}2107\text{ cm}^{-1}$) are observed in the complexes containing axial carbonyl ligands.

For characterization by mass spectrometry, MALDI-TOF spectra gave unsatisfactory results. In contrast, clean ESI mass spectra were obtained, but the intact complexes could not be observed. The peaks of highest intensity



Scheme 1.

correspond to the fragment obtained after cleavage of the axial CO ligand(s) in **1** and **4**, while dimers of these fragments can also be observed with low intensities (Table 1). In the case of **2**, the base peak at $m/z = 679$ corresponds to the monomeric unit ($M/2 - \text{CO}$) of the postulated dimer; a fragment corresponding to a loss of one CO ligand from the dimeric unit appears with low intensity ($M - \text{CO} + \text{Na}$). The thermogravimetric analysis (TGA) of **1** and **2** shows

a correlation with the ESI-MS behavior. For **1**, the TGA curve at 210–245 °C shows a mass loss corresponding to two CO molecules. For **2**, a mass loss is observed in the range 188–282 °C which corresponds to a loss of two CO molecules from the tetranuclear complex or of one CO molecule from one half of the coordination dimer.

The ^{13}C NMR chemical shifts of **1**–**5** are also given in Table 1. The axial CO ligands can be clearly distinguished

Table 1
Selected IR, MS and NMR data of complexes **1–5**

	1	2	3	4	5
IR ^a : $\nu(\text{CO})$ [cm ⁻¹]	2107 vs, 2083 vs, 2075 s, 2042 s, 2025 vs, 2007 vs	2099 vs, 2042 vs, 2021 vs, 2011 s, 1948 s	2046 vs, 1996 m, 1956 vs	2086 s, 2034 vs, 1998 s, 1963 m, 1935 w	2035 s, 1996 m, 1965 s
MS (ESI) ^b , m/z	703 (100%, M–2CO+Na), 1381 (2 × (M–2CO)+Na)	679 (100%, M/2–CO), 702 (M/2)–CO+Na), 1432 (M–CO+2Na)	–	965 (100%, M–CO+Na), 1904 (2 × (M–CO)+Na)	–
¹³ C NMR ^c					
$\delta(\text{CO}_{\text{eq}})$	195.8, 197.3	197.3, 201.8	A ^d : 200.13, 201.19 B ^d : 199.36, 201.53	198.1 (d, $J_{\text{C,P}} = 2.9$), 203.2 (d, $J_{\text{C,P}} = 5.1$) 181.1 (d, $^3J_{\text{C,P}} = 32.9$)	202.5 (vt ^e , $J = 3.3$), 204.0 (vt, $J = 4.8$)
$\delta(\text{CO}_{\text{ax}})$	179.05	175.5	A: 120.21, 124.10, 129.15, 133.06, 133.17, 142.30, 175.85 (NCO) B: 120.53, 123.77, 129.09, 132.78, 133.10, 142.68, 176.30 (NCO)	178.9 (d, $J_{\text{C,P}} = 8.8$) (NCO)	178.6 (vt, $J = 6.2$) (NCO)
$\delta(\text{sac})$	121.1 (CH), 124.6 (CH), 128.5 (C), 133.8 (CH), 134.0 (CH), 139.9 (C), 178.95 (NCO)	122.0, 124.4, 129.6, 133.9, 134.7, 142.8, 176.7 (NCO)	A: 3.57 (CH ₃ CN), 122.97 (CN) B: 4.16 (CH ₃ CN)		
Other signals					
³¹ P NMR ^c				22.0	14.1

^a KBr pellets; vs = very strong, s = strong, m = medium, w = weak.

^b Only the highest peak of the multiplet of isotope peaks is given, assignment in parentheses (M = molecular mass).

^c Solvent: C₂D₂Cl₄ for **1**, [D₈]-THF for **2**, CDCl₃ for **3–5**.

^d A mixture of two isomers was obtained, **3A:3B** ≈ 2.5:1.

^e vt = virtual triplet.

from the equatorial ones. On the other hand, the ^{13}C data do not allow a systematic distinction between head–head and head–tail isomers. The spectra of **3**, where both isomers are present, illustrate that the chemical shifts of all corresponding signals are very close. Due to the low solubility of **2** in non-donor solvents, the ^{13}C spectra of this complex was recorded in $[\text{D}_8]\text{-THF}$, and therefore, the data most likely represent those of $[\text{Ru}_2(\mu\text{-sac})_2(\text{CO})_5(\text{thf})]$.

2.2. Solid-state structures of **1**, **3A**, **4** and **5**

The structures of **1**, **3A**, **4**, and **5** were established by X-ray single crystal structure analysis (Figs. 1–4). In three cases, solvent of crystallization was incorporated in the crystal: **3A** \times *p*-xylene, **4** \times CH_2Cl_2 and **5** \times $3\text{CH}_2\text{Cl}_2$. In all cases, a “sawhorse” arrangement, with a *cis* relationship of the two saccharinate ligands at each metal center, is observed which is characteristic for dinuclear complexes of the general composition $[\text{Ru}_2(\text{CO})_4(\mu\text{-L})_2]$ (for examples, see literature [12,18,19,21,23,25]). The saccharinate units act as bidentate ligands via their amidate ($\text{N}-\text{C}=\text{O}$) moiety. In **1**, **3A** and **5** they bridge the two ruthenium atoms in a head–tail (or 1,1) fashion. The axial positions at both metal atoms are occupied by CO (in **1**), acetonitrile (in **3A**), or PPh_3 (in **5**) ligands. Thus, these dinuclear complexes have an overall C_2 topology which in the case of **3A** coincides with a crystallographic C_2 -axis. Compound **3A** crystallizes with one *p*-xylene molecule per formula unit; the

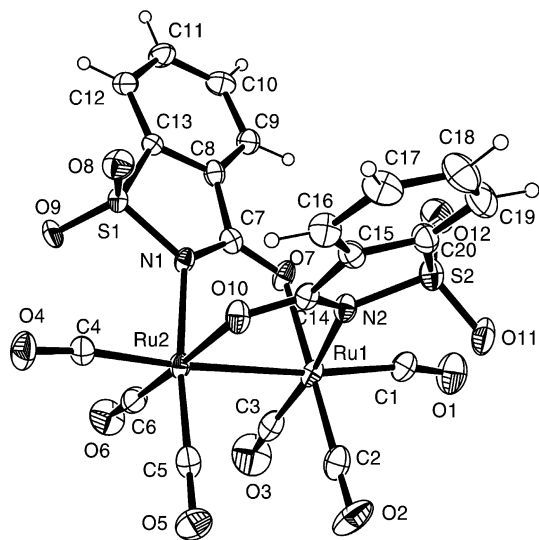


Fig. 1. Structure of **1** in the solid state; ellipsoids of thermal vibration are shown at 30% probability. Selected bond lengths (Å) and angles ($^\circ$): Ru1–Ru2 2.7713(9), Ru1–N2 2.156(6), Ru1–O7 2.137(5), Ru1–C1 2.002(9), Ru1–C2 1.889(9), Ru1–C3 1.891(9), C1–O1 1.117(10), C2–O2 1.119(10), C3–O3 1.141(10), Ru2–N1 2.134(6), Ru2–O10 2.126(5), Ru2–C4 1.989(8), Ru2–C5 1.868(9), Ru2–C6 1.850(8), C4–O4 1.117(9), C5–O5 1.170(9), C6–O6 1.153(9), O7–C7 1.259(8), C7–N1 1.325(10), O10–C14 1.264(9), C14–N2 1.319(9); N2–Ru1–O7 86.3(2), N1–Ru2–O10 86.9(2), Ru2–Ru1–C1 173.3(2), Ru1–C1–O1 169.6(8), Ru1–Ru2–C4 174.7(2), Ru2–C4–O4 171.8(7); N2–Ru1–Ru2–O10 $-9.3(2)$, N1–Ru2–Ru1–O7 $-8.6(2)$, C2–Ru1–Ru2–C5 $-7.4(3)$.

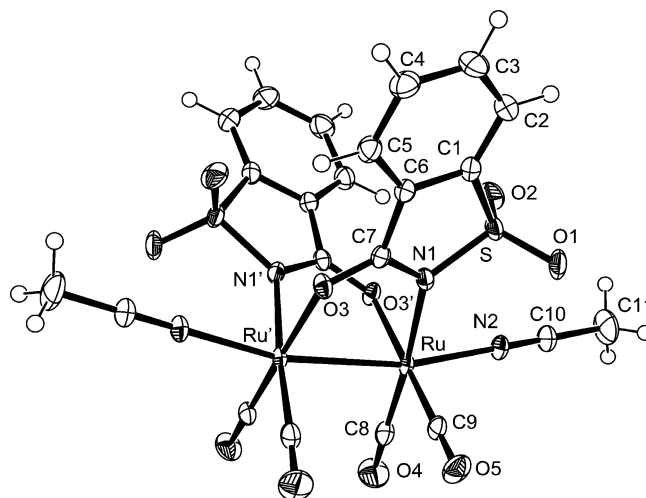


Fig. 2. Structure of **3A** in the solid state; ellipsoids of thermal vibration are shown at 50% probability. The *p*-xylene solvate molecule is not shown. Selected bond lengths (Å) and angles ($^\circ$): Ru–Ru' 2.7113(4), Ru–N1 2.154(2), Ru–O3' 2.136(2), Ru–N2 2.149(2), Ru–C8 1.862(3), Ru–C9 1.841(3), C8–O4 1.137(4), C9–O5 1.143(3), N1–C7 1.347(3), C7–O3 1.248(3), S–O1 1.433(2), S–O2 1.429(2), N2–O10 1.130(3); N1–Ru–O3' 84.46(8), Ru–Ru–N1 81.24(5), Ru–Ru–O3' 86.50(4), Ru–Ru–N2 167.51(6), Ru–N2–C10 179.5(2); N1–Ru–Ru'–O3' $-11.6(2)$, C9–Ru–Ru'–C8' $-11.8(2)$. Atoms marked with a prime are generated by the symmetry operation: $-x + 1, y, -z + 0.5$.

p-xylene molecule also has crystallographic C_2 symmetry with both methyl carbons positioned on the rotation axis (i.e., the methyl hydrogen atoms are positionally disordered over two symmetry-related sites).

Complex **4**, in contrast to **1**, **3A** and **5**, has the head–head arrangement of the two sac ligands, and the sterically less accessible axial coordination site (neighbored by two SO_2 groups) is occupied by the small CO ligand. The torsion angles around the Ru–Ru axis show that the in-plane rotation of the equatorial coordination plane containing Ru2 relative to that containing Ru1 is larger than in the head–tail complexes.

In three of the four complexes, remarkably long Ru–Ru distances are found (**1**: 2.7713(9) Å; **3A**: 2.7113(4) Å; **4**: 2.7754(5) Å; **5**: 2.7725(5) and 2.7747(5) Å) which are larger than in similar dinuclear Ru(I,I) complexes with amidate or pyridin-2-olate bidentate bridging ligands and various axial ligands, such as in the following examples: 2.688(1) Å in $[\text{Ru}_2(\mu\text{-HNC}(\text{Ph})\text{O})_2(\text{CH}_3\text{CN})_2(\text{CO})_2]$ [25a], 2.609–2.710 Å in complexes with pyridin-2-olate ligands [21,26,27]. A comparison of the Ru–Ru distance in **1** and **3** shows that the strongly coordinating axial CO ligands cause a significant bond lengthening as compared to acetonitrile ligands. It is also informative to compare the metal–metal distance in **1** with that in other diruthenium(I,I) hexacarbonyl complexes such as $[\text{Ru}_2(\mu\text{-OOCPh})_2(\text{CO})_6]$ (2.704(1) Å) [23b], $[\text{Ru}_2(\mu\text{-3,5-dimethylpyrazolate})_2(\text{CO})_6]$ (2.705(2) Å) [18], and $[\text{Ru}_2(\mu\text{-ArNNNAr})_2(\text{CO})_6]$ (Ar = 4-chlorophenyl) (2.6701(6) Å) [12]. It is evident that the saccharinate ligands contribute considerably to the stretching of the Ru–Ru bond. Cotton et al. [17] have made

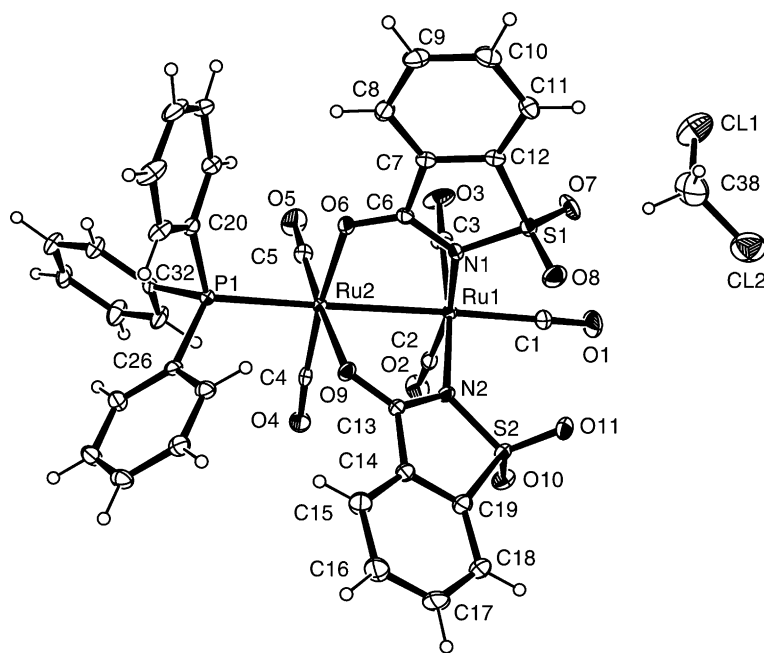


Fig. 3. Structure of $4 \times \text{CH}_2\text{Cl}_2$ in the solid state; ellipsoids of thermal vibration are shown at 30% probability. Selected bond lengths (Å) and angles (°): Ru1–Ru2 2.7754(5), Ru1–N1 2.149(2), Ru1–N2 2.119(2), Ru1–C1 2.003(3), Ru1–C2 1.878(3), Ru1–C3 1.872(3), C1–O1 1.115(4), C2–O2 1.141(4), C3–O3 1.135(4), Ru2–O6 2.128(2), Ru2–O9 2.162(2), Ru2–C4 1.842(3), Ru2–C5 1.842(3), Ru2–P1 2.431(1); Ru2–Ru1–C1 174.79(9), N1–Ru1–Ru2 79.67(6), Ru1–Ru2–P1 173.12(2), O6–Ru2–O9 88.45(8); N1–Ru1–Ru2–O6 15.42(8), N2–Ru1–Ru2–O9 16.19(8), C2–Ru1–Ru2–C4 21.25(13). Closest intermolecular contact of the dichloromethane molecule: C38–O7 3.284(5) Å, H38A–O7 2.67 Å, C38–H38a–O7 120.7°.

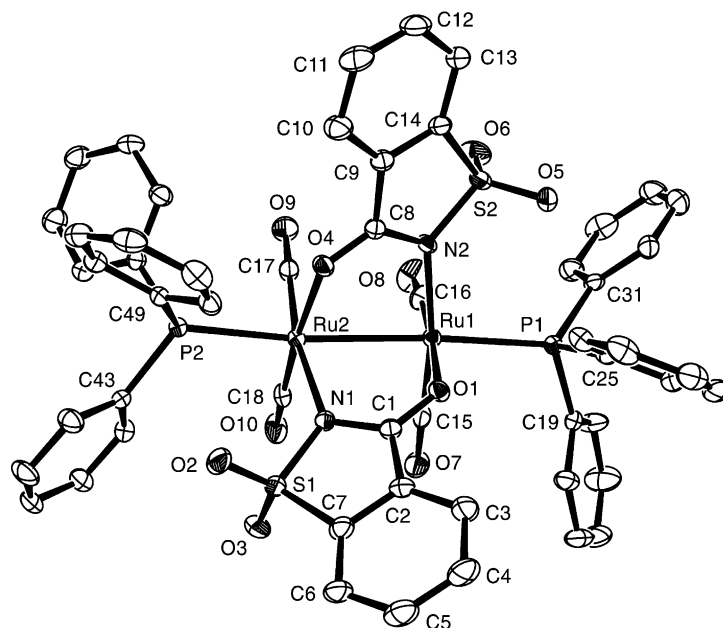
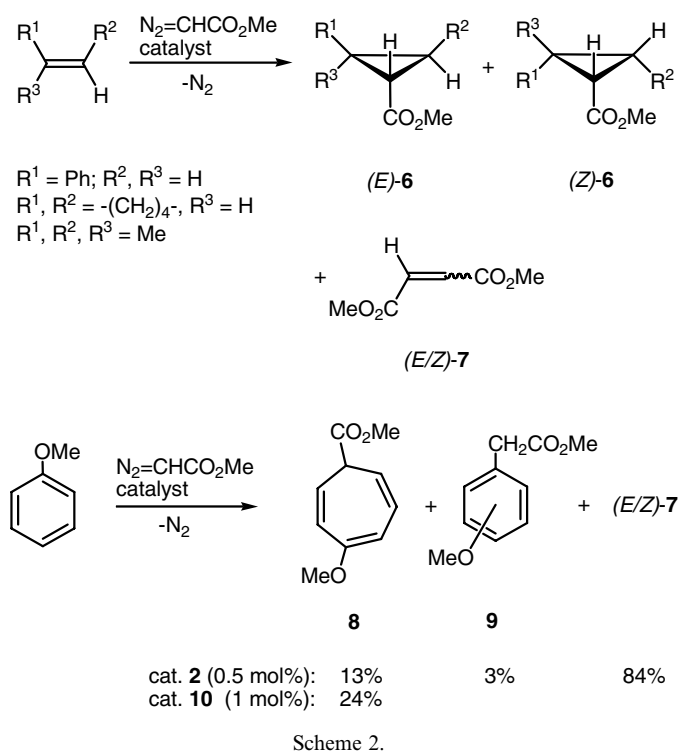


Fig. 4. Structure of **5** in the solid state; ellipsoids of thermal vibration are shown at 30% probability. Only one of the two molecules in the asymmetric unit is shown and the dichloromethane solvate molecules as well as the hydrogen atoms are omitted. Selected bond lengths (Å) and angles (°): Ru1–Ru2 2.7725(5), Ru1–O1 2.148(3), Ru1–N2 2.166(4), Ru1–P1 2.462(1), Ru1–C15 1.861(5), Ru1–C16 1.834(6), C15–O7 1.148(6), C16–O8 1.153(6), N2–C8 1.339(5), N2–S2 1.656(4), C8–O4 1.246(6), Ru2–O4 2.146(3), Ru2–N1 2.163(4), Ru2–P2 2.470(1), Ru2–C17 1.852(6), Ru2–C18 1.840(5), C17–O9 1.152(6), C18–O10 1.159(6), N1–C1 1.345(6), N1–S1 1.666(4), C1–O1 1.266(6); Ru2–Ru1–P1 169.96(3), Ru2–Ru1–N2 81.21(8), Ru2–Ru1–O1 82.40(7), O1–Ru1–N2 88.45(2); O1–Ru1–Ru2–N1 19.2(2), Ru1–Ru2–P2 169.16(3), N2–Ru1–Ru2–O4 19.0(2), C15–Ru1–Ru2–C18 21.6(2).

similar observations on the dinuclear chromium complexes $[\text{Cr}_2(\text{sac})_4\text{L}_2]$ (L = thf, pyridine) and have suggested that the effect could be related in part to the high acidity of the parent saccharin ligand.

2.3. Ru-catalyzed carbene transfer reactions

Complexes **1** and **2** were tested for their ability to catalyze carbene transfer from methyl diazoacetate (MDA) to



olefins and arenes (Scheme 2). Styrene, cyclohexene, and 2-methyl-2-butene were chosen as the olefinic substrates because they represent different electronic and steric conditions and the results can be compared with our preceding investigations using related ruthenium catalysts. The reactions were carried out by slow addition of MDA to a large excess of the liquid olefin diluted with CH_2Cl_2 and containing the catalyst. While complex **1** was well soluble in the alkene- CH_2Cl_2 phase, complex **2** dissolved completely only after addition of a small amount of MDA, indicating the cleavage of the coordination dimer of **2** by the diazoester. After the addition of MDA was completed, it took several hours before all the diazoester had been consumed. While the reaction times increased from styrene to 2-methyl-2-butene, a clear-cut and general difference between the performance of catalysts **1** and **2** could not be observed. Yields of cyclopropanes *E/Z*-**6** and the formal carbene dimers dimethyl fumarate and maleate (*E/Z*-**7**) are given in Table

2. It was found that for the three alkenes, the yields of cyclopropanation catalyzed by **1** or **2** are in general a little lower than with $[\text{Ru}_2(\mu\text{-OAc})_2(\text{CO})_4]_n$ (**10**, entry 4) under the same conditions [10a], but they compare favorably with other catalysts of this type bearing carboxylate [10,11], triazenide [12] and 2-pyridonate [11] ligands. Initially, we had expected that the presence of the SO_2 group in the ligands would enhance the electrophilicity of catalysts **1** and **2**, with a concomitant increased ability for the diazo decomposition reaction and increased efficiency and effectiveness as cyclopropanation catalysts. These expectations are not met by the results shown in Table 2 and disagree with the considerably longer reaction times for the more highly substituted alkenes, which due to their nucleophilicity should be more susceptible to reaction with an electrophilic metal-carbene intermediate ($\text{L}_n\text{Ru}=\text{CHCO}_2\text{Me}$). The relative slowness of the reactions could be caused by catalyst deactivation (competitive coordination of olefin or reaction products instead of the diazo compound), but an increase of the amount of catalyst **2** from 1 to 3 mol% (entries 2 and 3) did not lead to major improvement. On the other hand, when the amount of 2-methyl-2-butene was reduced by a factor of 10 (i.e., equimolar amounts of diazoacetate and olefin were involved in the reaction), the reaction time for complete consumption of MDA after its addition to the alkene/catalyst phase decreased from 6 to 2 h (catalyst **2**), but the yield of cyclopropanes *E/Z*-**6** went down to 20% while the yield of *E/Z*-**7** increased to 37%. This indicates that the diazoester competes strongly with the olefin for the ruthenium-carbene intermediate. The diastereoselectivities of the cyclopropanation reactions are in the expected ranges [10–12], but the increased *Z*- (or *syn*-) selectivity with catalyst **1**, similar to related ruthenium triazenide complexes [12], merits attention.

Similar to complex **10** [10a], the saccharinato-ruthenium complexes reported here are not suited for proficient intermolecular carbene transfer to arenes. Thus, decomposition of MDA in neat benzene catalyzed by **2** does not give a carbene addition product. When the more electron-rich anisole was used as substrate and solvent, the cycloheptatrienecarboxylate **8** and the isomeric (methoxyphenyl)acetate **9** were obtained in a combined yield of 16% (Scheme 2), somewhat less than with **10** as catalyst. The low yield may be due in part to the

Table 2
Cyclopropanation of alkenes with methyl diazoacetate (MDA) in CH_2Cl_2 ^a

Entry	Catalyst	Catalyst loading (mol%)	Yields of cyclopropanes 6 [%, relative to MDA] (<i>E/Z</i> or <i>anti/syn</i> ratio) ^b		
			From styrene	From cyclohexene	From 2-methyl-2-butene
1	$[\text{Ru}_2(\mu\text{-sac})_2(\text{CO})_6]$ (1)	1	62 (1.0)	45 (1.1)	43 (0.13)
2	$[\text{Ru}_2(\mu\text{-sac})_2(\text{CO})_5]_2$ (2)	1	76 (1.8)	60 (1.5)	46 (0.20)
3	$[\text{Ru}_2(\mu\text{-sac})_2(\text{CO})_5]_2$ (2)	3	69 (2.0)	61 (2.7)	61 (0.26)
4	$[\text{Ru}_2(\mu\text{-OAc})_2(\text{CO})_4]_n$ (10)	1	95 (1.6)	68 (3.7)	61 (0.16)

^a Conditions: see Section 4.3.1.

^b Dimers *E/Z*-**7** (~1:1) were also formed in all cases. Yield of *E/Z*-**7** (%): entry 1: styrene 11, cyclohexene 28, 2-methyl-2-butene 14; entry 2: styrene 7, cyclohexene 22, 2-methyl-2-butene 16; entry 3: styrene 11, cyclohexene 21, 2-methyl-2-butene 13; and entry 4: not determined.

insufficient amount of catalyst (0.5 mol%) which was dictated, however, by the low solubility of **2** in anisole. In contrast to the alkene cyclopropanation reactions described above, the solubility of **2** did not improve even after complete addition of the diazoester.

3. Conclusion

Dinuclear Ru_2^{2+} complexes of the type $[\text{Ru}_2(\mu\text{-L}^1)_2(\text{CO})_4\text{L}_2^2]$ where L^1 is a bridging saccharinate ligand can easily be synthesized from $\text{Ru}_3(\text{CO})_{12}$ and saccharin and are very stable towards air and moisture. Depending on the axial ligands (CO, CH_3CN , PPh_3), they are obtained with a head–head or a head–tail arrangement of the two saccharinate ligands or as a mixture of isomers. Contrary to expectation, the presence of electron-withdrawing SO_2 groups in the saccharinate ligands does not enhance the efficiency of these complexes for decomposition of diazoacetic esters compared to, e.g., the related acetate complexes $[\text{Ru}_2(\mu\text{-OAc})_2(\text{CO})_4\text{L}_2]$. Nevertheless, $[\text{Ru}_2(\mu\text{-sac})_2(\text{CO})_6]$ (**1**) and $[\text{Ru}_2(\mu\text{-sac})_2(\text{CO})_5]_2$ (**2**) were found to be suitable catalysts for the cyclopropanation of nucleophilic olefins with methyl diazoacetate. The yields compare favorably with those obtained with related Ru_2^{2+} complexes bearing carboxylate, triazenide and 2-pyridonate bridging ligands, and catalyst **1** induces a higher diastereoselectivity for *Z(syn)*-cyclopropanes than $[\text{Ru}_2(\mu\text{-OAc})_2(\text{CO})_4]_n$.

4. Experimental

4.1. General remarks

NMR spectra: Bruker DRX 400 (^1H : 400.13 MHz; ^{13}C : 100.62 MHz; ^{31}P : 161.98 MHz); the solvent signal was used as the internal standard for the ^1H and ^{13}C spectra (CDCl_3 : $\delta_{\text{H}} = 7.26$, $\delta_{\text{C}} = 77.0$ ppm; THF: $\delta_{\text{H}} = 1.72$ ppm; $[1,2\text{-D}_2]$ -tetrachloroethane: $\delta_{\text{C}} = 73.7$ ppm), while the δ_{P} values are referenced to external H_3PO_4 ($\delta_{\text{P}} = 0$ ppm). – IR spectra: Bruker Vector 22. – Mass spectra, ESI: Waters micro-mass ZMD. – Elemental analyses: Elementar Vario EL. TGA: Mettler Toledo TGA/SDTA851, heating rate $10^\circ\text{C}/\text{min}$, N_2 flow (50 ml/min). – GC: Varian CP-3800 with a FID. $\text{Ru}_3(\text{CO})_{12}$ [28] and methyl diazoacetate [29] were prepared by published procedures. All reactions were performed under an inert atmosphere (argon) and in dry solvents.

4.2. Preparation of ruthenium complexes

4.2.1. Hexacarbonyl- $1\kappa^3\text{C}:2\kappa^3\text{C}$ -(μ -saccharinato- $1\kappa\text{O}:2\kappa\text{N}$)-(μ -saccharinato- $1\kappa\text{N}:2\kappa\text{O}$)-diruthenium-(Ru–Ru), $[\text{Ru}_2(\mu\text{-sac})_2(\text{CO})_6]$ (**1**)

A solution of $\text{Ru}_3(\text{CO})_{12}$ (300 mg, 0.47 mmol) and saccharin (258 mg, 1.40 mmol) in toluene (30 ml) was heated at 90°C (bath temperature) for 36 h. The pale yellow precipitate was filtered off, washed with ether (5 ml) and pentane (5 ml), then dried at 0.001 mbar/ 20°C for 4 h. Yield:

415 mg (0.57 mmol, 80% based on $\text{Ru}_3(\text{CO})_{12}$). Decomposition of the complex, indicated by a color change to red and brown, started above 200°C . IR (KBr): 2107 vs, 2083 vs, 2075 s, 2042 s, 2025 vs, 2007 vs, 1616 m, 1585 m, 1380 m, 1328 m, 1177 m, 1167 m cm^{-1} . ^1H NMR (CDCl_3): $\delta = 7.66\text{--}7.73$ (m, 4H), 7.81 (dd, 2H), 7.87 (dd, 2H). Anal. Calc. for $\text{C}_{20}\text{H}_8\text{N}_2\text{O}_{12}\text{Ru}_2\text{S}_2$ (734.5): C, 32.70; H, 1.10; N, 3.81. Found: C, 32.55; H, 1.14; N, 3.75%.

4.2.2. $[\text{Ru}_2(\mu\text{-sac})_2(\text{CO})_5]_2$ (**2**)

A solution of $\text{Ru}_3(\text{CO})_{12}$ (250 mg, 0.39 mmol) and saccharin (215 mg, 1.17 mmol) in toluene (40 ml) was heated at reflux for 5 h. After 30 min a yellow solid began to precipitate. The suspension was concentrated to about 20 ml and cooled to 7°C , then the solid was filtered off and washed with diethylether and pentane (5 ml each). The yellow powder was dried at $160^\circ\text{C}/0.02$ mbar for 4 h, but residual toluene was still present after this treatment. Yield of **2**: 367 mg (0.26 mmol, 89%). Decomposition of the complex, indicated by a color change to brown and black, started above 210°C . IR (KBr): 2099 vs, 2042 vs, 2021 vs, 2011 s, 1948 s, 1615 m, 1584 m, 1333 m, 1314 s, 1180 m, 1148 m cm^{-1} . ^1H NMR ($[\text{D}_8]$ -THF): $\delta = 2.30$ and $7.06\text{--}7.20$ (residual toluene solvent, 0.04 mol%), $7.64\text{--}7.94$ (m, all H-sac). Anal. Calc. for $\text{C}_{38}\text{H}_{16}\text{N}_4\text{O}_{22}\text{Ru}_4\text{S}_4$ (1413.1): C, 32.30; H, 1.14; N, 3.96. Found: C, 32.55; H, 1.30; N, 3.82%. $\text{C}_{38}\text{H}_{16}\text{N}_4\text{O}_{22}\text{Ru}_4\text{S}_4 \times 0.04$ toluene requires: C, 32.45; H, 1.16; N, 3.95.

4.2.3. $[\text{Ru}_2(\mu\text{-sac})_2(\text{CH}_3\text{CN})_2(\text{CO})_4]$ (**3**)

Method 1. Complex **2** (33 mg) was dissolved in boiling acetonitrile (4 ml). The solvent was evaporated and the yellow powder of **3** was dried for 1 h at $45^\circ\text{C}/20$ mbar. Decomposition of the complex, indicated by a color change to brown, started above 215°C . According to the NMR spectra, a mixture of two species (**3A**, **B**) is present in solution, **A**:**B** ≈ 2.9 :1 at 295 K. IR (KBr): 2315 vw, 2288 vw, 2046 vs, 1996 m, 1956 vs, 1618 m, 1583 m, 1465 m, 1374 m, 1362 m, 1320 m, 1176 m, 1164 m, 1129 w cm^{-1} . ^1H NMR (CDCl_3): $\delta = 2.40$ (s, CH_3CN , major species **A**), 2.44 (s, CH_3CN , minor species **B**), 7.57–7.87 (several m, H-sac, **A** and **B**). Anal. Calc. for $\text{C}_{22}\text{H}_{18}\text{N}_4\text{O}_{10}\text{Ru}_2\text{S}_2$ (760.6): C, 34.74; H, 1.86; N, 7.37. Found: C, 34.68; H, 2.01; N, 7.33%. – Crystallization of **3** from $\text{CH}_3\text{CN}/p$ -xylene afforded yellow crystals of bis(acetonitrile)- $1\kappa\text{N}:2\kappa\text{N}$ -tetracarbonyl- $1\kappa^2\text{C}:2\kappa^2\text{C}$ -(μ -saccharinato- $1\kappa\text{N}:2\kappa\text{O}$)-(μ -saccharinato- $1\kappa\text{O}:2\kappa\text{N}$)-diruthenium(Ru–Ru) (**3A**).

Method 2. A suspension of **1** (63 mg, 86 μmol) in CH_3CN (2 ml) was stirred at 50°C until a clear yellow solution had formed. After cooling at r.t., the solvent was evaporated, the residue was dissolved in dichloromethane (2 ml), and pentane was added until the solution became turbid (ca. 6 ml). The mixture was kept at -30°C for two days, and the precipitate was collected and dried ($45^\circ\text{C}/20$ mbar); yellow solid (60 mg, 92%). The NMR spectra were identical to those of the product obtained by method 1.

4.2.4. *Pentacarbonyl-1κ³C:2κ²C-bis(μ-saccharinato-1κN:2κO)-triphenylphosphane-2κP-diruthenium(Ru–Ru), [Ru₂(μ-sac)₂(CO)₅(PPh₃)] (4) and tetracarbonyl-1κ²C:2κ²C-(μ-saccharinato-1κO:2κN)-(μ-saccharinato-1κN:2κO)-bis(triphenylphosphane-1κP:2κP-diruthenium(Ru–Ru), [Ru₂(μ-sac)₂(CO)₄(PPh₃)₂] (5)*

Method 1. Dichloromethane (5 ml) was added to complex **1** (82 mg, 112 μmol) and triphenylphosphane (59 mg, 224 μmol) at 20 °C. An orange solution was obtained within a few minutes and gas evolution was observed. After 10 min, the solvent was removed at 40 °C/15 mbar. In order to remove excess PPh₃, the residue was suspended in cyclohexane (10 ml) and treated with ultrasound during 10 min. A solid was isolated by centrifugation and was dried at 110 °C/0.001 mbar for 24 h; yield: 117 mg. It consisted of a yellow and an orange component which could be separated manually and were identified as **4** and **5**, respectively. It was observed that the orange solid deposited faster than the yellow one from the suspension in cyclohexane. The original ratio of **4**:**5** was 1:5 (³¹P NMR integration).

Method 2. Dichloromethane (5 ml) was added to complex **2** (40 mg, 28 μmol) and triphenylphosphane (31 mg, 118 μmol) at 20 °C. An orange solution was gradually formed and after 15 min, the solvent was removed at 40 °C/15 mbar. Further workup as described above provided 52 mg of a mixture of **4** and **5** (1:28 by ³¹P NMR integration).

Spectroscopic and analytical data of **4**: IR (CH₂Cl₂ film on NaCl plate): 3062 w, 2086 s, 2034 vs, 1998 s, 1963 m, 1935 w, 1616 s, 1584 s, 1436 m, 1387 m, 1331 s, 1178 s, 1126 m, 1094 m cm⁻¹. ¹H NMR (CDCl₃): δ = 6.98 (d, *J*_{H,H} = 7.6 Hz, 2H), 7.45–7.50 (m, 8H), 7.52–7.56 (m, 3H), 7.59 (d, *J*_{H,H} = 1.5 Hz, 2H), 7.60–7.64 (m, 6H), 7.79 (d, *J*_{H,H} = 7.8 Hz, 2H). ¹³C{¹H} NMR (CDCl₃): δ = 121.4, 123.6, 128.7, 128.8, 129.5, 130.5 (d, *J*_{C,P} = 2.2 Hz), 131.5, 131.9, 133.0, 133.3, 133.6, 133.7, 141.2, 178.9 (d, *J*_{C,P} = 8.8 Hz), 181.1 (d, ³*J*_{C,P} = 32.9 Hz), 198.1 (d, *J*_{C,P} = 2.9 Hz), 203.2 (d, *J*_{C,P} = 5.1 Hz). ³¹P (CDCl₃): δ = 22.0.

Spectroscopic and analytical data of **5**: IR (CH₂Cl₂ film on NaCl plate): 3060 w, 2035 s, 1996 s, 1965 s, 1614 s, 1579 s, 1435 m, 1380 m, 1330 s, 1176 s cm⁻¹. ¹H NMR (CDCl₃): δ = 7.06 (d, *J*_{H,H} = 7.6 Hz, 2H), 7.37–7.41 (m, 17H), 7.44–7.48 (m, 3H), 7.56–7.62 (m, 4H), 7.64–7.69 (m, 12H). ¹³C{¹H} NMR (CDCl₃): δ = 120.8, 123.7, 128.0 (vt, *J* = 4.8 Hz), 128.4, 128.5, 128.7, 129.7, 129.7, 132.2, 132.9, 133.1, 134.2 (vt, *J* = 5.9 Hz), 134.4, 134.5, 142.4, 178.6 (vt, *J* = 6.2 Hz), 202.5 (vt, *J* = 3.3 Hz), 204.0 (vt, *J* = 4.8 Hz) (vt = virtual triplet). ³¹P (CDCl₃): δ = 14.1.

4.3. Catalytic carbene transfer reactions

4.3.1. Method A: cyclopropanation of alkenes

The catalyst was suspended at r.t. in a mixture of alkene (9 mmol) and dry dichloromethane (4 ml). By means of a

syringe pump, a solution of methyl diazoacetate (0.10 g, 1 mmol) in dry dichloromethane and alkene (1 mmol) was added during 4 h (10 h in the case of 2-methyl-2-butene). Then, the reaction mixture was stirred until complete consumption of the diazo compound was indicated by IR ($\nu(\text{C}=\text{N}_2) = 2115 \text{ cm}^{-1}$) (from 5 h to more than 20 h). The solution was passed through a short silica gel column to remove the catalyst, and a defined amount of naphthalene (for experiments with styrene and cyclohexene) or mesitylene (for 2-methyl-2-butene) was added to the eluate as an internal standard. The yields and diastereomer ratios of cyclopropanes were determined by GC, using a Varian CP-WAX 52 column (30 m × 0.32 mm, film thickness 0.25 μm) fitted with a retention gap. The response factor of each cyclopropane diastereomer was determined on samples prepared separately.

4.3.2. Method B: reaction with arenes

A solution of methyl diazoacetate (2.00 g, 20 mmol) in the liquid arene (20 mmol) was added at r.t. during 26 h, by means of a syringe pump, to a solution of the same arene (180 mmol) containing 0.5 mol% of catalyst. Complete disappearance of the diazo compound was observed after 44–70 h (IR control). Products were isolated by column chromatography on silica gel (100 g, Merck silica gel 60, 0.063–0.200 mm). Successive elution with pentane, ether/pentane mixtures, and diethyl ether furnished excess arene, products **8/9**, and a mixture of dimethyl fumarate and dimethyl maleate (*E/Z*-7). All products are known; they were identified by their ¹H NMR spectra [30] and their yields were determined by product isolation or from the crude product mixture by ¹H NMR integration, using naphthalene as the internal standard.

4.4. X-ray crystal structure determination for **1**, **3A**, **4**, and **5**

Single crystals of **1** were obtained by slow evaporation of a dichloromethane solution, but the crystal quality was rather poor. Crystals of **3A** × *p*-xylene were obtained by slow evaporation of an acetonitrile/*p*-xylene solution at r.t. Crystals of **4** × CH₂Cl₂ and **5** × 3CH₂Cl₂ were obtained from dichloromethane/pentane by a diffusion method, starting from a **4/5** mixture. The crystals of **4** (yellow) and **5** (orange) were separated manually. In the latter case, the crystals were isolated and immediately coated with an oil and cooled to prevent loss of solvent of crystallization which would cause degradation of the crystals within a few minutes. Data collection was performed on an image-plate diffractometer (Stoe IPDS) using monochromated Mo Kα radiation ($\lambda = 0.71073 \text{ \AA}$). No absorption correction was applied. Structure solution was achieved by direct methods, and the structures were refined against *F*_o² values using a full-matrix least-squares method. Hydrogen atom positions were calculated geometrically and treated as riding on their bond neighbors in the refinement procedure. Software for structure solution and refinement: SHELX-97 [31]; molecule plots: ORTEP-3 [32]. Crystallographic data

Table 3
Summary of crystallographic data and structure refinement for compounds **1**, **3A**, **4**, and **5**

Compound	1	3A	4	5
Empirical formula	C ₂₀ H ₈ N ₂ O ₁₂ Ru ₂ S ₂	C ₂₂ H ₁₄ N ₄ O ₁₀ Ru ₂ S ₂ × C ₈ H ₁₀ ^a	C ₃₇ H ₂₃ N ₂ O ₁₁ Ru ₂ S ₂ × CH ₂ Cl ₂ ^b	C ₅₄ H ₃₈ N ₂ O ₁₀ Ru ₂ S ₂ × 3CH ₂ Cl ₂ ^b
Formula weight	734.54	760.64 + 106.16	937.86 + 84.95	1203.12 + 254.80
<i>T</i> (K)	295(2)	173(2)	193(2)	220(2)
Crystal size (mm)	0.38 × 0.31 × 0.38	0.54 × 0.23 × 0.08	0.54 × 0.38 × 0.27	0.43 × 0.43 × 0.39
Crystal system	Monoclinic	Monoclinic	Triclinic	Monoclinic
Space group	<i>P</i> ₂ ₁ / <i>c</i>	<i>C</i> ₂ / <i>c</i>	<i>P</i> $\bar{1}$	<i>P</i> ₂ ₁ / <i>n</i>
<i>a</i> (Å)	7.886(1)	13.468(1)	12.876(2)	15.974(1)
<i>b</i> (Å)	14.760(1)	16.610(2)	13.378(2)	34.863(3)
<i>c</i> (Å)	21.367(3)	15.401(1)	13.535(2)	21.379(2)
α (°)	90	90	98.95(2)	90
β (°)	97.57(2)	106.32(2)	112.11(2)	93.25(1)
γ (°)	90	90	103.97(2)	90
<i>V</i> (Å ³)	2465.3(5)	3306.5(6)	2016.0(5)	11887.1(17)
<i>Z</i>	4	4	2	8
ρ_{ber} (g cm ⁻³)	1.979	1.741	1.736	1.629
μ (Mo K α) (cm ⁻¹)	14.62	11.02	10.87	0.96
θ Range (°)	2.37–23.99	2.16–25.95	2.39–26.00	1.94–24.13
Index ranges of <i>h</i> , <i>k</i> , <i>l</i>	–8/8, –16/16, –24/24	–15/16, –20/20, –18/17	–15/16, –16/16, –16/16	–18/18, –39/40, –24/24
Reflections collected	15159	12862	23873	76619
Independent reflections (<i>R</i> _{int})	3818 (0.1354)	3027 (0.0618)	7335 (0.0372)	18615 (0.0609)
Completeness to θ_{max} (%)	99.1	93.6	92.6	98.1
Data/restraints/parameters ^b	3818/0/343	3027/0/222	7335/0/523	18165/6 ^c /1478
Goodness-of-fit on <i>F</i> ²	0.911	0.963	1.069	0.802
Final <i>R</i> indices <i>R</i> ₁ , <i>wR</i> ₂ ^{c,d} [<i>I</i> > 2 σ (<i>I</i>)]	0.0527, 0.1082	0.0275, 0.0683	0.0257, 0.0658	0.0350, 0.0776
<i>R</i> indices <i>R</i> ₁ , <i>wR</i> ₂ ^{c,d} (all data)	0.0867, 0.1162	0.0337, 0.0703	0.0342, 0.0745	0.0729, 0.0814
Largest difference in peak and hole (e Å ⁻³)	0.76 and –0.75	0.63 and –1.345	1.19 and –0.90	0.80 and –0.90

^a *p*-Xylene solvate.

^b Dichloromethane solvate.

^c Refinement based on *F*² values.

^d $R_1 = \sum ||F_o| - |F_c|| / \sum |F_o|$; $wR_2 = [\sum (w(F_o^2 - F_c^2)^2) / \sum w(F_o^2)^2]^{1/2}$.

^e One CH₂Cl₂ molecule is disordered over two positions.

and details of the refinement for the four structures are given in Table 3.

Acknowledgments

This work has received financial support by the Deutsche Forschungsgemeinschaft. The support and sponsorship conceded by COST action D24 ‘Sustainable Chemical Processes: Stereoselective Transition Metal-Catalyzed Reactions’ is kindly acknowledged.

Appendix A. Supplementary material

CCDC-285843 (**1**), CCDC-285844 (**3A**), CCDC-295914 (**4**) and CCDC-295915 (**5**) contains the supplementary crystallographic data for this paper. These data can be obtained free of charge at www.ccdc.cam.ac.uk/conts/retrieving.html [or from the Cambridge Crystallographic Data Centre, 12, Union Road, Cambridge CB2 1EZ, UK; fax: (internat.) +44 1223 336 033; e-mail: deposit@ccdc.cam.ac.uk]. Supplementary data associated with this article can be found, in the online version, at [doi:10.1016/j.jorganchem.2006.02.013](https://doi.org/10.1016/j.jorganchem.2006.02.013).

References

- [1] M.P. Doyle, M.A. McKervey, T. Ye, *Modern Catalytic Methods for Organic Synthesis with Diazo Compounds: From Cyclopropanes to Ylides*, Wiley, New York, 1998.
- [2] (a) M.P. Doyle, D.C. Forbes, *Chem. Rev.* 98 (1998) 911–936; (b) H.M.L. Davies, R.E.J. Beckwith, *Chem. Rev.* 103 (2003) 2861–2903; (c) C.A. Merlic, A.L. Zechman, *Synthesis* (2003) 1137–1156.
- [3] G. Maas, *Chem. Soc. Rev.* 33 (2004) 183–190.
- [4] (a) S.-L. Zheng, W.-Y. Yu, C.-M. Che, *Org. Lett.* 4 (2002) 889–892; (b) W.-H. Cheung, S.-L. Zheng, W.-Y. Yu, G.-C. Zhou, C.-M. Che, *Org. Lett.* 5 (2003) 2535–2538; (c) M.K.-W. Choi, W.-Y. Yu, C.-M. Che, *Org. Lett.* 7 (2005) 1081–1084.
- [5] (a) S. Sengupta, D. Das, D.S. Sarma, *Tetrahedron Lett.* 37 (1996) 8815–8818; (b) E. Galardon, S. Roué, P. Le Maux, G. Simonneaux, *Tetrahedron Lett.* 39 (1998) 2333–2334; (c) F. Simal, A. Demonceau, A.F. Noels, *Tetrahedron Lett.* 40 (1999) 63–66; (d) E. Galardon, P. Le Maux, G. Simonneaux, *Tetrahedron* 56 (2000) 615–622; (e) R.P. Wurz, A.B. Charette, *Org. Lett.* 4 (2002) 4531–4533; (f) A. Del Zotto, W. Baratta, F. Miani, G. Verardo, P. Rigo, *Inorg. Chim. Acta* 349 (2003) 249–252.

- [6] (a) M. Alt, G. Maas, *Tetrahedron* 50 (1994) 7435–7444;
(b) C.-Y. Zhou, W.-Y. Yu, C.-M. Che, *Org. Lett.* 4 (2002) 3235–3238;
(c) C.-Y. Zhou, P.W.H. Chan, W.-Y. Yu, C.-M. Che, *Synthesis* (2003) 1403–1412.
- [7] (a) O. Fujimura, T. Honma, *Tetrahedron Lett.* 39 (1998) 625–626;
(b) Y. Chen, L. Huang, M.A. Ranade, X.P. Zhang, *J. Org. Chem.* 68 (2003) 3714–3717;
(c) F.E. Kühn, A.M. Santos, A.A. Jogalekar, F.M. Pedro, P. Rigo, W. Baratta, *J. Catal.* 227 (2004) 253–256.
- [8] A. Del Zotto, W. Baratta, F. Miani, G. Verardo, P. Rigo, *Eur. J. Org. Chem.* (2000) 3731–3735.
- [9] (a) J.P. Collman, E. Rose, G.D. Venburg, *J. Chem. Soc., Chem. Commun.* (1993) 934–935;
(b) W. Baratta, A. Del Zotto, P. Rigo, *Chem. Commun.* (1997) 2163–2164.
- [10] (a) G. Maas, T. Werle, M. Alt, D. Mayer, *Tetrahedron* 49 (1993) 881–888;
(b) G. Maas, J. Seitz, *Tetrahedron Lett.* 42 (2001) 6137–6140;
(c) T. Werle, G. Maas, *Adv. Synth. Catal.* 343 (2001) 37–40.
- [11] T. Werle, L. Schäffler, G. Maas, *J. Organomet. Chem.* 690 (2005) 5562–5569.
- [12] C.-D. Leger, G. Maas, *Z. Naturforsch. B* 59 (2004) 573–578.
- [13] See, for example: (a) L.R. Falvello, J. Gomez, I. Pascual, M. Tomás, E.P. Urriolabeitia, A.J. Schultz, *Inorg. Chem.* 40 (2001) 4455–4463;
(b) E.J. Baran, *Quim. Nova* 28 (2005) 326–328;
(c) V.T. Yilmaz, S. Guney, W.T.A. Harrison, *Z. Naturforsch. B* 60 (2005) 403–407;
(d) S. Hamamci, V.T. Yilmaz, W.T.A. Harrison, *Z. Naturforsch. B* 60 (2005) 978–983.
- [14] See, for example: (a) S.Z. Haider, K.M.A. Malik, K.J. Ahmed, H. Hess, H. Riffel, M.B. Hursthouse, *Inorg. Chim. Acta* 72 (1983) 21–27;
(b) F.A. Cotton, G.E. Lewis, C.A. Murillo, W. Schwotzer, G. Valle, *Inorg. Chem.* 23 (1984) 4038–4041.
- [15] (a) G. Jovanovski, A. Hergold-Brundić, B. Kamenar, *Acta Crystallogr., Sect. C* 44 (1988) 63–66;
(b) E.J. Baran, C.C. Wagner, M. Rossi, F. Caruso, *Z. Anorg. Allg. Chem.* 626 (2000) 701–705;
(c) V.T. Yilmaz, S. Guney, C. Thoene, *Z. Anorg. Allg. Chem.* 628 (2002) 1406–1410.
- [16] P. Naumov, G. Jovanovski, S.-Z. Hu, I.-H. Suh, I.A. Razak, S. Chantrapromma, H.-K. Fun, S.W. Ng, *Acta Crystallogr., Sect. C* 57 (2001) 1016–1019.
- [17] (a) F.A. Cotton, L.R. Falvello, W. Schwotzer, C.A. Murillo, G. Valle-Bourrouet, *Inorg. Chim. Acta* 190 (1991) 89–96;
(b) N.M. Alfaro, F.A. Cotton, L.M. Daniels, C.A. Murillo, *Inorg. Chem.* 31 (1992) 2718–2723.
- [18] (a) J.A. Cabeza, C. Landázuri, L.A. Oro, D. Belletti, A. Tiripicchio, M. Tiripicchio-Camellini, *J. Chem. Soc., Dalton Trans.* (1989) 1093–1100;
(b) J.A. Cabeza, C. Landázuri, L.A. Oro, A. Tiripicchio, M. Tiripicchio-Camellini, *J. Organomet. Chem.* 322 (1987) C16–C20.
- [19] P.L. Andreu, J.A. Cabeza, V. Riera, Y. Jeannin, D. Miguel, *J. Chem. Soc., Dalton Trans.* (1990) 2201–2206.
- [20] G.R. Crooks, B.F.G. Johnson, J. Lewis, I.G. Williams, *J. Chem. Soc.* (A) (1969) 2761–2766.
- [21] L. Schäffler, B. Müller, G. Maas, *Inorg. Chim. Acta* 359 (2006) 970–977.
- [22] L. Schäffler, G. Maas, unpublished results.
- [23] (a) H. Schumann, J. Opitz, J. Pickart, *J. Organomet. Chem.* 128 (1977) 253–264;
(b) M. Spohn, T. Vogt, J. Strähle, *Z. Naturforsch. B* 41 (1986) 1373–1380.
- [24] G. Süß-Fink, G. Herrmann, P. Morys, J. Ellermann, A. Veit, *J. Organomet. Chem.* 284 (1985) 263–273.
- [25] (a) F. Neumann, H. Stoeckli-Evans, G. Süß-Fink, *J. Organomet. Chem.* 379 (1989) 139–150;
(b) M. Rotem, I. Goldberg, U. Shmueli, Y. Shvo, *J. Organomet. Chem.* 314 (1986) 185–212.
- [26] P.L. Andreu, J.A. Cabeza, G.A. Carriedo, V. Riera, S. García-Granda, J.F. Van der Maelen, G. Mori, *J. Organomet. Chem.* 421 (1991) 305–314.
- [27] S.J. Sherlock, M. Cowie, E. Singleton, M.M. de V. Steyn, *J. Organomet. Chem.* 361 (1989) 353–367.
- [28] A. Mantovani, S. Ceni, *Inorg. Synth.* 16 (1976) 47–48.
- [29] (a) N.E. Searle, *Org. Synth. Coll. IV* (1963) 424–426;
(b) H.-U. Reißig, J. Reichelt, T. Kunz, *Org. Synth.* 71 (1992) 189–199.
- [30] (a) A.J. Anciaux, A. Demonceau, A.F. Noels, A.J. Hubert, R. Warin, P. Teyssié, *J. Org. Chem.* 46 (1981) 873–876;
(b) N. Mandava, H. Finegold, *Spectrosc. Lett.* 13 (1980) 59–68.
- [31] G.M. Sheldrick, *SHELX-97: Program for the Solution and Refinement of Crystal Structures from Diffraction Data*, University of Göttingen, Göttingen, Germany, 1997.
- [32] L.J. Farrugia, *J. Appl. Crystallogr.* 30 (1997) 565.